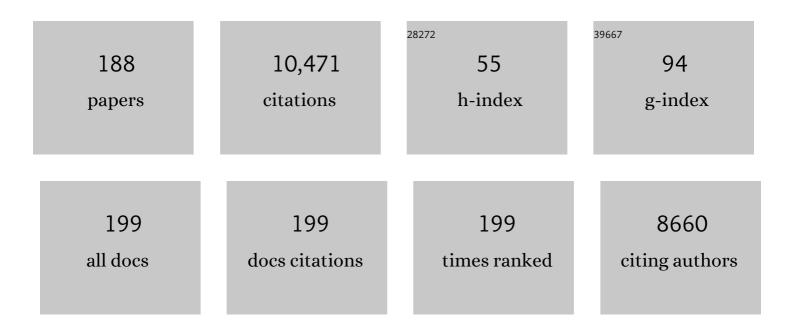


## List of Publications by Year in descending order

Source: https://exaly.com/author-pdf/599199/publications.pdf Version: 2024-02-01



XIN YANG

#	Article	IF	CITATIONS
1	Joint Landmark and Structure Learning for Automatic Evaluation of Developmental Dysplasia of the Hip. IEEE Journal of Biomedical and Health Informatics, 2022, 26, 345-358.	6.3	7
2	NasmamSR: a fast image super-resolution network based on neural architecture search and multiple attention mechanism. Multimedia Systems, 2022, 28, 321-334.	4.7	7
3	Cell Localization and Counting Using Direction Field Map. IEEE Journal of Biomedical and Health Informatics, 2022, 26, 359-368.	6.3	10
4	An improved anchor neighborhood regression SR method based on low-rank constraint. Visual Computer, 2022, 38, 405-418.	3.5	6
5	Fast Image Super-Resolution Based on Limit Gradient Embedding Cascaded Forest. Circuits, Systems, and Signal Processing, 2022, 41, 2007-2026.	2.0	2
6	An image super-resolution network based on multi-scale convolution fusion. Visual Computer, 2022, 38, 4307-4317.	3.5	10
7	Imitation Learning-Based Algorithm for Drone Cinematography System. IEEE Transactions on Cognitive and Developmental Systems, 2022, 14, 403-413.	3.8	2
8	Role of Antioxidant Moieties in the Quenching of a Purine Radical by Dissolved Organic Matter. Environmental Science & Technology, 2022, 56, 546-555.	10.0	19
9	A Novel UVA/ClO <sub>2</sub> Advanced Oxidation Process for the Degradation of Micropollutants in Water. Environmental Science & amp; Technology, 2022, 56, 1257-1266.	10.0	40
10	Convolutional apsule network for gastrointestinal endoscopy image classification. International Journal of Intelligent Systems, 2022, 37, 5796-5815.	5.7	17
11	DCU-net: a deformable convolutional neural network based on cascade U-net for retinal vessel segmentation. Multimedia Tools and Applications, 2022, 81, 15593-15607.	3.9	14
12	Ferroptosis-related long non-coding RNA signature predicts the prognosis of hepatocellular carcinoma. Aging, 2022, 14, 4069-4084.	3.1	13
13	Region Separable Stereo Matching. IEEE Transactions on Multimedia, 2022, , 1-14.	7.2	0
14	Lightweight image super-resolution with feature cheap convolution and attention mechanism. Cluster Computing, 2022, 25, 3977-3992.	5.0	7
15	The multiple roles of chlorite on the concentrations of radicals and ozone and formation of chlorate during UV photolysis of free chlorine. Water Research, 2021, 190, 116680.	11.3	36
16	Reactivity of Chlorine Radicals (Cl <sup>•</sup> and Cl <sub>2</sub> <sup>•–</sup> ) with Dissolved Organic Matter and the Formation of Chlorinated Byproducts. Environmental Science & Technology, 2021, 55, 689-699.	10.0	124
17	An image super-resolution deep learning network based on multi-level feature extraction module. Multimedia Tools and Applications, 2021, 80, 7063-7075.	3.9	12
18	3D-CNN-SPP: A Patient Risk Prediction System From Electronic Health Records via 3D CNN and Spatial Pyramid Pooling. IEEE Transactions on Emerging Topics in Computational Intelligence, 2021, 5, 247-261.	4.9	9

#	Article	IF	CITATIONS
19	Fast Depth Prediction and Obstacle Avoidance on a Monocular Drone Using Probabilistic Convolutional Neural Network. IEEE Transactions on Intelligent Transportation Systems, 2021, 22, 156-167.	8.0	39
20	A Set of Markers Related to Viral Infection Has a Sex-sensitive Prognostic Value in Papillary Thyroid Carcinoma. Journal of Clinical Endocrinology and Metabolism, 2021, 106, e2334-e2346.	3.6	2
21	Kinetics and Mechanisms of Virus Inactivation by Chlorine Dioxide in Water Treatment: A Review. Bulletin of Environmental Contamination and Toxicology, 2021, 106, 560-567.	2.7	30
22	miR-124 Alleviates Ischemic Stroke-Induced Neuronal Death by Targeting DAPK1 in Mice. Frontiers in Neuroscience, 2021, 15, 649982.	2.8	7
23	Effect of UV/chlorine treatment on photophysical and photochemical properties of dissolved organic matter. Water Research, 2021, 192, 116857.	11.3	34
24	Image super-resolution reconstruction based on improved Dirac residual network. Multidimensional Systems and Signal Processing, 2021, 32, 1065-1082.	2.6	10
25	Remote sensing image superâ€resolution based on convolutional blind denoising adaptive dense connection. IET Image Processing, 2021, 15, 2508-2520.	2.5	5
26	PARP inhibitors promote stromal fibroblast activation by enhancing CCL5 autocrine signaling in ovarian cancer. Npj Precision Oncology, 2021, 5, 49.	5.4	10
27	Retinal vessel segmentation based on an improved deep forest. International Journal of Imaging Systems and Technology, 2021, 31, 1792-1802.	4.1	7
28	Prediction of Photolysis Kinetics of Viral Genomes under UV254 Irradiation to Estimate Virus Infectivity Loss. Water Research, 2021, 198, 117165.	11.3	10
29	Variation-Aware Federated Learning With Multi-Source Decentralized Medical Image Data. IEEE Journal of Biomedical and Health Informatics, 2021, 25, 2615-2628.	6.3	59
30	UV254 irradiation of N-chloro-α-amino acids: Kinetics, mechanisms, and N-DBP formation potentials. Water Research, 2021, 199, 117204.	11.3	16
31	Roles and Knowledge Gaps of Point-of-Use Technologies for Mitigating Health Risks from Disinfection Byproducts in Tap Water: A Critical Review. Water Research, 2021, 200, 117265.	11.3	51
32	Rate Constants and Mechanisms for Reactions of Bromine Radicals with Trace Organic Contaminants. Environmental Science & Technology, 2021, 55, 10502-10513.	10.0	51
33	Radiation Oncologists' Perceptions of Adopting an Artificial Intelligence–Assisted Contouring Technology: Model Development and Questionnaire Study. Journal of Medical Internet Research, 2021, 23, e27122.	4.3	22
34	TAGLN mediated stiffness-regulated ovarian cancer progression via RhoA/ROCK pathway. Journal of Experimental and Clinical Cancer Research, 2021, 40, 292.	8.6	25
35	Image Super-Resolution Based on the Down-Sampling Iterative Module and Deep CNN. Circuits, Systems, and Signal Processing, 2021, 40, 3437-3455.	2.0	2
36	Robust and Efficient RGB-D SLAM in Dynamic Environments. IEEE Transactions on Multimedia, 2021, 23, 4208-4219.	7.2	13

#	Article	IF	CITATIONS
37	40 Hz Light Flicker Promotes Learning and Memory via Long Term Depression in Wild-Type Mice. Journal of Alzheimer's Disease, 2021, 84, 983-993.	2.6	13
38	Upregulation of CD22 by Chidamide promotes CAR T cells functionality. Scientific Reports, 2021, 11, 20637.	3.3	10
39	Redox-Active Moieties in Dissolved Organic Matter Accelerate the Degradation of Nitroimidazoles in SO <sub>4</sub> <sup>•–</sup> -Based Oxidation. Environmental Science & Technology, 2021, 55, 14844-14853.	10.0	35
40	Semi-supervised mp-MRI data synthesis with StitchLayer and auxiliary distance maximization. Medical Image Analysis, 2020, 59, 101565.	11.6	19
41	Oxidation of tetrabromobisphenol A (TBBPA) by peroxymonosulfate: The role of in-situ formed HOBr. Water Research, 2020, 169, 115202.	11.3	47
42	An improved target tracking algorithm based on spatio-temporal context under occlusions. Multidimensional Systems and Signal Processing, 2020, 31, 329-344.	2.6	4
43	Prediction of adsorption capacity for pharmaceuticals, personal care products and endocrine disrupting chemicals onto various adsorbent materials. Chemosphere, 2020, 238, 124658.	8.2	35
44	Bi-Modality Medical Image Synthesis Using Semi-Supervised Sequential Generative Adversarial Networks. IEEE Journal of Biomedical and Health Informatics, 2020, 24, 855-865.	6.3	36
45	A new TLD target tracking method based on improved correlation filter and adaptive scale. Visual Computer, 2020, 36, 1783-1795.	3.5	11
46	Gallic acid accelerated BDE47 degradation in PMS/Fe(III) system: Oxidation intermediates autocatalyzed redox cycling of iron. Chemical Engineering Journal, 2020, 384, 123248.	12.7	64
47	Coexposure Degradation of Purine Derivatives in the Sulfate Radical-Mediated Oxidation Process. Environmental Science & Technology, 2020, 54, 1186-1195.	10.0	26
48	A Review on Hexachloro-1,3-butadiene (HCBD): Sources, Occurrence, Toxicity and Transformation. Bulletin of Environmental Contamination and Toxicology, 2020, 104, 1-7.	2.7	4
49	Intelligent bearing fault diagnosis using PCA–DBN framework. Neural Computing and Applications, 2020, 32, 10773-10781.	5.6	82
50	ClO2 pre-oxidation impacts the formation and nitrogen origins of dichloroacetonitrile and dichloroacetamide during subsequent chloramination. Water Research, 2020, 186, 116313.	11.3	13
51	Natural polyphenols enhanced the Cu(II)/peroxymonosulfate (PMS) oxidation: The contribution of Cu(III) and HO•. Water Research, 2020, 186, 116326.	11.3	117
52	Copper Inhibition of Triplet-Sensitized Phototransformation of Phenolic and Amine Contaminants. Environmental Science & Technology, 2020, 54, 9980-9989.	10.0	22
53	DoFE: Domain-Oriented Feature Embedding for Generalizable Fundus Image Segmentation on Unseen Datasets. IEEE Transactions on Medical Imaging, 2020, 39, 4237-4248.	8.9	59
54	The reactions of chlorine dioxide with inorganic and organic compounds in water treatment: kinetics and mechanisms. Environmental Science: Water Research and Technology, 2020, 6, 2287-2312.	2.4	50

#	Article	IF	CITATIONS
55	Discovering the Importance of ClO <sup>•</sup> in a Coupled Electrochemical System for the Simultaneous Removal of Carbon and Nitrogen from Secondary Coking Wastewater Effluent. Environmental Science & Technology, 2020, 54, 9015-9024.	10.0	76
56	DENAO: Monocular Depth Estimation Network with Auxiliary Optical Flow. IEEE Transactions on Pattern Analysis and Machine Intelligence, 2020, 43, 1-1.	13.9	8
57	Multi-Task Siamese Network for Retinal Artery/Vein Separation via Deep Convolution Along Vessel. IEEE Transactions on Medical Imaging, 2020, 39, 2904-2919.	8.9	20
58	Metformin Ameliorates Synaptic Defects in a Mouse Model of AD by Inhibiting Cdk5 Activity. Frontiers in Cellular Neuroscience, 2020, 14, 170.	3.7	34
59	Rarely seen primary cardiac natural killer/T cell lymphoma: a case report. Translational Cancer Research, 2020, 9, 394-399.	1.0	2
60	Enabling a Single Deep Learning Model for Accurate Gland Instance Segmentation: A Shape-Aware Adversarial Learning Framework. IEEE Transactions on Medical Imaging, 2020, 39, 2176-2189.	8.9	29
61	Exploration of reaction rates of chlorine dioxide with tryptophan residue in oligopeptides and proteins. Journal of Environmental Sciences, 2020, 93, 129-136.	6.1	7
62	Outcomes of patients with pelvic leiomyosarcoma treated by surgery and relevant auxiliary diagnosis. World Journal of Clinical Cases, 2020, 8, 1887-1896.	0.8	2
63	D <sup>2</sup> VO: Monocular Deep Direct Visual Odometry. , 2020, , .		2
64	Real-Time Dense Monocular SLAM With Online Adapted Depth Prediction Network. IEEE Transactions on Multimedia, 2019, 21, 470-483.	7.2	36
65	Real-Time Semantic Plane Reconstruction on a Monocular Drone Using Sparse Fusion. IEEE Transactions on Vehicular Technology, 2019, 68, 7383-7391.	6.3	9
66	Disinfection byproducts and their toxicity in wastewater effluents treated by the mixing oxidant of ClO2/Cl2. Water Research, 2019, 162, 471-481.	11.3	70
67	Betulinic Acid Induces ROS-Dependent Apoptosis and S-Phase Arrest by Inhibiting the NF- <i>κ</i> B Pathway in Human Multiple Myeloma. Oxidative Medicine and Cellular Longevity, 2019, 2019, 1-14.	4.0	35
68	Degradation and DBP formations from pyrimidines and purines bases during sequential or simultaneous use of UV and chlorine. Water Research, 2019, 165, 115023.	11.3	32
69	Learning to Capture a Film-Look Video with a Camera Drone. , 2019, , .		24
70	Rate Constants and Mechanisms of the Reactions of Cl <sup>•</sup> and Cl <sub>2</sub> <sup>•–</sup> with Trace Organic Contaminants. Environmental Science & Technology, 2019, 53, 11170-11182.	10.0	277
71	Heterotypic CAF-tumor spheroids promote early peritoneal metastasis of ovarian cancer. Journal of Experimental Medicine, 2019, 216, 688-703.	8.5	145
72	Synergistic removal of ammonium by monochloramine photolysis. Water Research, 2019, 152, 226-233.	11.3	56

#	Article	IF	CITATIONS
73	Transformation of adenine and cytosine in chlorination — An ESI-tqMS investigation. Chemosphere, 2019, 234, 505-512.	8.2	12
74	Different biotransformation of three hexabromocyclododecane diastereoisomers by Pseudomonas sp. under aerobic conditions. Chemical Engineering Journal, 2019, 374, 870-879.	12.7	17
75	Photochemical oxidation of PPCPs using a combination of solar irradiation and free available chlorine. Science of the Total Environment, 2019, 682, 629-638.	8.0	52
76	Enhanced removal of Cr(VI) in the Fe(III)/natural polyphenols system: role of the in situ generated Fe(II). Journal of Hazardous Materials, 2019, 377, 321-329.	12.4	49
77	Chlorite formation during ClO2 oxidation of model compounds having various functional groups and humic substances. Water Research, 2019, 159, 348-357.	11.3	62
78	Combining solar irradiation with chlorination enhances the photochemical decomposition of microcystin-LR. Water Research, 2019, 159, 324-332.	11.3	36
79	The influence of the UV/chlorine advanced oxidation of natural organic matter for micropollutant degradation on the formation of DBPs and toxicity during post-chlorination. Chemical Engineering Journal, 2019, 373, 870-879.	12.7	50
80	Bayesian DeNet: Monocular Depth Prediction and Frame-Wise Fusion With Synchronized Uncertainty. IEEE Transactions on Multimedia, 2019, 21, 2701-2713.	7.2	32
81	Effects of KMnO4/NaHSO3 pre-oxidation on the formation potential of disinfection by-products during subsequent chlorination. Chemical Engineering Journal, 2019, 372, 825-835.	12.7	22
82	Mechanical cues modulate cellular uptake of nanoparticles in cancer via clathrin-mediated and caveolae-mediated endocytosis pathways. Nanomedicine, 2019, 14, 613-626.	3.3	17
83	Visual-Inertial State Estimation with Pre-integration Correction for Robust Mobile Augmented Reality. , 2019, , .		8
84	Targeting INHBA in Ovarian Cancer Cells Suppresses Cancer Xenograft Growth by Attenuating Stromal Fibroblast Activation. Disease Markers, 2019, 2019, 1-13.	1.3	20
85	CAR T Cell Therapy for Hematological Malignancies. Current Medical Science, 2019, 39, 874-882.	1.8	22
86	Influence of (photo)bromination on the transformation, aggregation and sedimentation of graphene oxide. Chemical Engineering Journal, 2019, 355, 487-497.	12.7	13
87	Reactive obstacle avoidance of monocular quadrotors with online adapted depth prediction network. Neurocomputing, 2019, 325, 142-158.	5.9	24
88	A Three-Stage Deep Learning Model for Accurate Retinal Vessel Segmentation. IEEE Journal of Biomedical and Health Informatics, 2019, 23, 1427-1436.	6.3	244
89	ClO2 pre-oxidation changes the yields and formation pathways of chloroform and chloral hydrate from phenolic precursors during chlorination. Water Research, 2019, 148, 250-260.	11.3	38
90	Three-dimensional α-Fe2O3/amino-functionalization carbon nanotube sponge for adsorption and oxidative removal of tetrabromobisphenol A. Separation and Purification Technology, 2019, 211, 359-367.	7.9	36

#	Article	IF	CITATIONS
91	Elimination kinetics and detoxification mechanisms of microcystin-LR during UV/Chlorine process. Chemosphere, 2019, 214, 702-709.	8.2	39
92	Combating Uncertainty with Novel Losses for Automatic Left Atrium Segmentation. Lecture Notes in Computer Science, 2019, , 246-254.	1.3	11
93	Multiline treatment of advanced squamous cell carcinoma of the lung: A case report and review of the literature. World Journal of Clinical Cases, 2019, 7, 1899-1907.	0.8	15
94	Targeting YAP suppresses ovarian cancer progression through regulation of the PI3K/Akt/mTOR pathway. Oncology Reports, 2019, 42, 2768-2776.	2.6	20
95	Joint Segment-Level and Pixel-Wise Losses for Deep Learning Based Retinal Vessel Segmentation. IEEE Transactions on Biomedical Engineering, 2018, 65, 1912-1923.	4.2	309
96	Differential UV–vis absorbance can characterize the reaction of organic matter with ClO2. Water Research, 2018, 139, 442-449.	11.3	35
97	Automated Detection of Clinically Significant Prostate Cancer in mp-MRI Images Based on an End-to-End Deep Neural Network. IEEE Transactions on Medical Imaging, 2018, 37, 1127-1139.	8.9	105
98	The Multiple Role of Bromide Ion in PPCPs Degradation under UV/Chlorine Treatment. Environmental Science & Technology, 2018, 52, 1806-1816.	10.0	157
99	Copper Inhibition of Triplet-Induced Reactions Involving Natural Organic Matter. Environmental Science & Technology, 2018, 52, 2742-2750.	10.0	36
100	Cu(II)-catalyzed degradation of ampicillin: effect of pH and dissolved oxygen. Environmental Science and Pollution Research, 2018, 25, 4279-4288.	5.3	19
101	Sorption, mobility, and bioavailability of PBDEs in the agricultural soils: Roles of co-existing metals, dissolved organic matter, and fertilizers. Science of the Total Environment, 2018, 619-620, 1153-1162.	8.0	23
102	Removal of chlorinated organic solvents from hydraulic fracturing wastewater by bare and entrapped nanoscale zero-valent iron. Chemosphere, 2018, 196, 9-17.	8.2	45
103	Metformin Suppresses Tumor Progression by Inactivating Stromal Fibroblasts in Ovarian Cancer. Molecular Cancer Therapeutics, 2018, 17, 1291-1302.	4.1	67
104	Occurrence and indicators of pharmaceuticals in Chinese streams: A nationwide study. Environmental Pollution, 2018, 236, 889-898.	7.5	90
105	Robust and real-time pose tracking for augmented reality on mobile devices. Multimedia Tools and Applications, 2018, 77, 6607-6628.	3.9	12
106	Dicer reprograms stromal fibroblasts to a pro-inflammatory and tumor-promoting phenotype in ovarian cancer. Cancer Letters, 2018, 415, 20-29.	7.2	14
107	A Skeletal Similarity Metric for Quality Evaluation of Retinal Vessel Segmentation. IEEE Transactions on Medical Imaging, 2018, 37, 1045-1057.	8.9	38
108	Expression of BC1 Impairs Spatial Learning and Memory in Alzheimer's Disease Via APP Translation. Molecular Neurobiology, 2018, 55, 6007-6020.	4.0	43

#	Article	IF	CITATIONS
109	A Novel MicroRNA-124/PTPN1 Signal Pathway Mediates Synaptic and Memory Deficits in Alzheimer's Disease. Biological Psychiatry, 2018, 83, 395-405.	1.3	153
110	Through-the-Lens Drone Filming. , 2018, , .		20
111	A Deep Model with Shape-Preserving Loss for Gland Instance Segmentation. Lecture Notes in Computer Science, 2018, , 138-146.	1.3	25
112	ACT: An Autonomous Drone Cinematography System for Action Scenes. , 2018, , .		43
113	Monocular Camera Based Real-Time Dense Mapping Using Generative Adversarial Network. , 2018, , .		7
114	Bromide and Other Halide Ion Removal From Drinking Waters Using Silverâ€Amended Coagulation. Journal - American Water Works Association, 2018, 110, 13-24.	0.3	4
115	Accurate face alignment and adaptive patch selection for heart rate estimation from videos under realistic scenarios. PLoS ONE, 2018, 13, e0197275.	2.5	8
116	Extended adaptive event-triggered formation tracking control of a class of multi-agent systems with time-varying delay. Neurocomputing, 2018, 316, 386-398.	5.9	23
117	Impact of metal ions, metal oxides, and nanoparticles on the formation of disinfection byproducts during chlorination. Chemical Engineering Journal, 2017, 317, 777-792.	12.7	75
118	Degradation of 2,2′,4,4′-tetrabromodiphenyl ether (BDE-47) by a nano zerovalent iron-activated persulfate process: The effect of metal ions. Chemical Engineering Journal, 2017, 317, 613-622.	12.7	57
119	Automated diagnosis of prostate cancer in multi-parametric MRI based on multimodal convolutional neural networks. Physics in Medicine and Biology, 2017, 62, 6497-6514.	3.0	122
120	UV/chlorine treatment of carbamazepine: Transformation products and their formation kinetics. Water Research, 2017, 116, 254-265.	11.3	125
121	Defining the molecular properties of N-nitrosodimethylamine (NDMA) precursors using computational chemistry. Environmental Science: Water Research and Technology, 2017, 3, 502-512.	2.4	9
122	An automated method for accurate vessel segmentation. Physics in Medicine and Biology, 2017, 62, 3757-3778.	3.0	17
123	Co-trained convolutional neural networks for automated detection of prostate cancer in multi-parametric MRI. Medical Image Analysis, 2017, 42, 212-227.	11.6	115
124	Factors affecting the roles of reactive species in the degradation of micropollutants by the UV/chlorine process. Water Research, 2017, 126, 351-360.	11.3	263
125	Occurrence of nitrogenous and carbonaceous disinfection byproducts in drinking water distributed in Shenzhen, China. Chemosphere, 2017, 188, 257-264.	8.2	60
126	Radical Chemistry and Structural Relationships of PPCP Degradation by UV/Chlorine Treatment in Simulated Drinking Water. Environmental Science & amp; Technology, 2017, 51, 10431-10439.	10.0	449

#	Article	IF	CITATIONS
127	Real-time Monocular Dense Mapping for Augmented Reality. , 2017, , .		6
128	DBP formation from degradation of DEET and ibuprofen by UV/chlorine process and subsequent post-chlorination. Journal of Environmental Sciences, 2017, 58, 146-154.	6.1	33
129	Surface-modified biochar in a bioretention system for Escherichia coli removal from stormwater. Chemosphere, 2017, 169, 89-98.	8.2	107
130	Selective dissolution followed by EDDS washing of an e-waste contaminated soil: Extraction efficiency, fate of residual metals, and impact on soil environment. Chemosphere, 2017, 166, 489-496.	8.2	94
131	Photosensitized degradation of acetaminophen in natural organic matter solutions: The role of triplet states and oxygen. Water Research, 2017, 109, 266-273.	11.3	112
132	Reprogramming of stromal fibroblasts by SNAI2 contributes to tumor desmoplasia and ovarian cancer progression. Molecular Cancer, 2017, 16, 163.	19.2	47
133	Targeting Leptin as a Therapeutic Strategy against Ovarian Cancer Peritoneal Metastasis. Anti-Cancer Agents in Medicinal Chemistry, 2017, 17, 1093-1101.	1.7	22
134	MARCKS contributes to stromal cancer-associated fibroblast activation and facilitates ovarian cancer metastasis. Oncotarget, 2016, 7, 37649-37663.	1.8	30
135	β-Amyloid triggers aberrant over-scaling of homeostatic synaptic plasticity. Acta Neuropathologica Communications, 2016, 4, 131.	5.2	35
136	Fragments-based object tracking using probabilistic graphical model. , 2016, , .		1
137	Mechanisms and kinetics study on the trihalomethanes formation with carbon nanoparticle precursors. Chemosphere, 2016, 154, 391-397.	8.2	25
138	The photodegradation of polybrominated diphenyl ethers (PBDEs) in various environmental matrices: Kinetics and mechanisms. Chemical Engineering Journal, 2016, 297, 74-96.	12.7	88
139	PPCP degradation by UV/chlorine treatment and its impact on DBP formation potential in real waters. Water Research, 2016, 98, 309-318.	11.3	186
140	Characteristics and DBP formation of dissolved organic matter from leachates of fresh and aged leaf litter. Chemosphere, 2016, 152, 335-344.	8.2	18
141	Roles of reactive chlorine species in trimethoprim degradation in the UV/chlorine process: Kinetics and transformation pathways. Water Research, 2016, 104, 272-282.	11.3	267
142	Emerging investigators series: disinfection by-products in mixed chlorine dioxide and chlorine water treatment. Environmental Science: Water Research and Technology, 2016, 2, 838-847.	2.4	20
143	Integrating EDDS-enhanced washing with low-cost stabilization of metal-contaminated soil from an e-waste recycling site. Chemosphere, 2016, 159, 426-432.	8.2	65
144	Accurate and efficient pulse measurement from facial videos on smartphones. , 2016, , .		4

#	Article	IF	CITATIONS
145	Therapeutic Intervention of Learning and Memory Decays by Salidroside Stimulation of Neurogenesis in Aging. Molecular Neurobiology, 2016, 53, 851-866.	4.0	36
146	Infralimbic Endothelin1 Is Critical for the Modulation of Anxiety-Like Behaviors. Molecular Neurobiology, 2016, 53, 2054-2064.	4.0	2
147	The roles of halides in the acetaminophen degradation by UV/H2O2 treatment: Kinetics, mechanisms, and products analysis. Chemical Engineering Journal, 2015, 271, 214-222.	12.7	80
148	A Novel Mechanism of Spine Damages in Stroke via DAPK1 and Tau. Cerebral Cortex, 2015, 25, 4559-4571.	2.9	70
149	Effect of pH on the formation of disinfection byproducts in ferrate(VI) pre-oxidation and subsequent chlorination. Separation and Purification Technology, 2015, 156, 980-986.	7.9	33
150	Application of Pretreatment Methods for Reliable Dissolved Organic Nitrogen Analysis in Water—A Review. Critical Reviews in Environmental Science and Technology, 2015, 45, 249-276.	12.8	20
151	Ciprofloxacin adsorption on graphene and granular activated carbon: kinetics, isotherms, and effects of solution chemistry. Environmental Technology (United Kingdom), 2015, 36, 3094-3102.	2.2	84
152	Accurate Vessel Segmentation with Progressive Contrast Enhancement and Canny Refinement. Lecture Notes in Computer Science, 2015, , 1-16.	1.3	3
153	Investigation of disinfection byproducts formation in ferrate(VI) pre-oxidation of NOM and its model compounds followed by chlorination. Journal of Hazardous Materials, 2015, 292, 197-204.	12.4	97
154	Role of Chlorine Dioxide in <i>N</i> -Nitrosodimethylamine Formation from Oxidation of Model Amines. Environmental Science & Technology, 2015, 49, 11429-11437.	10.0	28
155	Sorption performance and mechanism of a sludge-derived char as porous carbon-based hybrid adsorbent for benzene derivatives in aqueous solution. Journal of Hazardous Materials, 2014, 274, 205-211.	12.4	56
156	Electrospray Ionization-Tandem Mass Spectrometry Method for Differentiating Chlorine Substitution in Disinfection Byproduct Formation. Environmental Science & amp; Technology, 2014, 48, 4877-4884.	10.0	29
157	Intervention of Death-Associated Protein Kinase 1–p53 Interaction Exerts the Therapeutic Effects Against Stroke. Stroke, 2014, 45, 3089-3091.	2.0	34
158	Factors affecting the formation of iodo-trihalomethanes during oxidation with chlorine dioxide. Journal of Hazardous Materials, 2014, 264, 91-97.	12.4	11
159	Pinning Cluster Synchronization for Delayed Dynamical Networks via Kronecker Product. Circuits, Systems, and Signal Processing, 2013, 32, 1907-1929.	2.0	18
160	Identifying the sources and fate of anthropogenically impacted dissolved organic matter (DOM) in urbanized rivers. Water Research, 2013, 47, 5027-5039.	11.3	165
161	Effluent Particle Size and Permeability of Polyvinylchloride Membranes after Sodium Hypochlorite Exposure. Journal of Environmental Engineering, ASCE, 2013, 139, 712-718.	1.4	4
162	The occurrence of disinfection by-products in municipal drinking water in China's Pearl River Delta and a multipathway cancer risk assessment. Science of the Total Environment, 2013, 447, 108-115.	8.0	72

#	Article	IF	CITATIONS
163	Effect of Suspended Solids on the Sequential Disinfection of Secondary Effluent by UV Irradiation and Chlorination. Journal of Environmental Engineering, ASCE, 2013, 139, 1482-1487.	1.4	17
164	Occurrence and fate of PPCPs and correlations with water quality parameters in urban riverine waters of the Pearl River Delta, South China. Environmental Science and Pollution Research, 2013, 20, 5864-5875.	5.3	87
165	Formation of disinfection byproducts upon chlorine dioxide preoxidation followed by chlorination or chloramination of natural organic matter. Chemosphere, 2013, 91, 1477-1485.	8.2	120
166	Formation of disinfection by-products after pre-oxidation with chlorine dioxide or ferrate. Water Research, 2013, 47, 5856-5864.	11.3	90
167	Nitrogen Origins and the Role of Ozonation in the Formation of Haloacetonitriles and Halonitromethanes in Chlorine Water Treatment. Environmental Science & Technology, 2012, 46, 12832-12838.	10.0	41
168	Effects of ozone and ozone/peroxide pretreatments on disinfection byproduct formation during subsequent chlorination and chloramination. Journal of Hazardous Materials, 2012, 239-240, 348-354.	12.4	57
169	Precursors and nitrogen origins of trichloronitromethane and dichloroacetonitrile during chlorination/chloramination. Chemosphere, 2012, 88, 25-32.	8.2	144
170	Effects of UV irradiation and UV/chlorine co-exposure on natural organic matter in water. Science of the Total Environment, 2012, 414, 576-584.	8.0	45
171	Occurrence and removal of pharmaceuticals and personal care products (PPCPs) in an advanced wastewater reclamation plant. Water Research, 2011, 45, 5218-5228.	11.3	450
172	Formation of halogenated organic byproducts during medium-pressure UV and chlorine coexposure of model compounds, NOM and bromide. Water Research, 2011, 45, 6545-6554.	11.3	76
173	Formation of disinfection byproducts from chlor(am)ination of algal organic matter. Journal of Hazardous Materials, 2011, 197, 378-388.	12.4	100
174	Ageing of polyvinylchloride membranes in ultrafiltration of drinking water by chemical cleaning. , 2011, , .		1
175	Removal of natural organic matter using surfactant-modified iron oxide-coated sand. Journal of Hazardous Materials, 2010, 174, 567-572.	12.4	39
176	Formation of carbonaceous and nitrogenous disinfection by-products from the chlorination of Microcystis aeruginosa. Water Research, 2010, 44, 1934-1940.	11.3	252
177	Nitrogenous disinfection byproducts formation and nitrogen origin exploration during chloramination of nitrogenous organic compounds. Water Research, 2010, 44, 2691-2702.	11.3	148
178	Characterization of algal organic matter and formation of DBPs from chlor(am)ination. Water Research, 2010, 44, 5897-5906.	11.3	327
179	Design and Reduction of UML-PN Models of Power Plant's Fault Management System. , 2009, , .		0
180	Classification and Recognition of Character Using WP Decomposition, Zernike Moments and Fuzzy		1

Integral. , 2009, , .

#	Article	IF	CITATIONS
181	Correlations between organic matter properties and DBP formation during chloramination. Water Research, 2008, 42, 2329-2339.	11.3	132
182	Factors affecting formation of haloacetonitriles, haloketones, chloropicrin and cyanogen halides during chloramination. Water Research, 2007, 41, 1193-1200.	11.3	229
183	Comparison of colorimetric and membrane introduction mass spectrometry techniques for chloramine analysis. Water Research, 2007, 41, 3097-3102.	11.3	62
184	THM, HAA and CNCl formation from UV irradiation and chlor(am)ination of selected organic waters. Water Research, 2006, 40, 2033-2043.	11.3	105
185	Quantification of aqueous cyanogen chloride and cyanogen bromide in environmental samples by MIMS. Water Research, 2005, 39, 1709-1718.	11.3	37
186	Kinetics of cyanogen chloride destruction by chemical reduction methods. Water Research, 2005, 39, 2114-2124.	11.3	12
187	DBP formation in breakpoint chlorination of wastewater. Water Research, 2005, 39, 4755-4767.	11.3	110
188	Chlorination Byproduct Formation in the Presence of Humic Acid, Model Nitrogenous Organic Compounds, Ammonia, and Bromide. Environmental Science & Technology, 2004, 38, 4995-5001.	10.0	113